Journal of Advanced Ceramics
2016, **5**(4): 277–283
DOI: 10.1007/s40145-016-0200-6

ISSN 2226-4108
CN 10-1154/TQ

Research Article

A new sintering approach to ceramics at low temperature from $Ba(Zr_xTi_{1-x})O_3$ nanoparticles doped by ZnO

Rui GUO[a], Jianquan QI[a,*], Jiali LUO[a], Xiaoyu DONG[a], Longtu LI[b]

[a]*School of Nature Resources & Materials Science*, *Northeastern University at Qinhuangdao*, *Qinhuangdao*, *Hebei 066004*, *China*
[b]*State Key Laboratory of Fine Ceramics and New Processing*, *Tsinghua University*, *Beijing 100084*, *China*

Received: May 25, 2016; Revised: July 12, 2016; Accepted: July 15, 2016

Abstract: The sintering temperature decreases theoretically with the grain size of the ceramic powders, but it is not always right for fine grain sized nanopowders due to the inevitable agglomerations, and thus pores are hard to eliminate thoroughly during sintering. To overcome this difficulty, a new approach is designed to sintering ceramics at low temperature from nanoparticles. In this scheme, excessive dopants, such as ZnO, are synthesized into the nanoparticles, and they would be liberated again on the surfaces of the grains at high temperature as sintering aids homogenously to promote densification. Here, we compared the ceramic sintering of ZnO-doped barium zirconate titanate ($BaZr_xTi_{1-x}O_3$, BZT) nanoparticles with BZT nanoparticles using ZnO as additive at 1150 ℃. Both kinds of nanoparticles were directly synthesized by the same process at room temperature and yielded the same initial grain size of ~10 nm. The dense BZT ceramic with relative density of 99% was fabricated from the 2 mol% ZnO-doped nanoparticles. On the other hand, the porous BZT ceramic with density of 78% was obtained from nanoparticles with 2 mol% ZnO as additive. Therefore, our strategy to ceramic sintering at low temperature from nanoparticles was confirmed.

Keywords: barium zirconate titanate ($BaZr_xTi_{1-x}O_3$, BZT); nanopowder; direct synthesis; sintering

1 Introduction

Sintering is a key point during ceramic processing for both structural and functional ceramics. At least, a kind of mass transfer must be occurred during ceramic sintering accompanying with pore exclusion from green wares, grain growth in ceramic body, and densification of ceramic production. According to the style of mass transfer, ceramic sintering can have several patterns as solid state sintering, liquid phase sintering, vapor-deposition sintering, reaction sintering, etc., in series. It is always important for the decrease of ceramic sintering temperature due to energy saving, co-firing of the ceramics with multiple ingredients, the necessity of certain inner electrodes for multiple layer functional ceramics, and so on. Both adding sintering aids in the ingredients and decreasing initial grain size of the ceramic powders are effective to lower sintering temperature [1–3]. In general, the sintering temperature theoretically decreases with the grain size of the ceramic powders. There are so many efforts on synthesis of perovskite structured nanoparticles to reduce the initial grain size and promote their sintering activity. Most perovskite phases are still prepared by conventional solid state reactions between the

* Corresponding author.
E-mail: jianquanqi@mail.tsinghua.edu.cn

corresponding oxides or oxides and carbonates at temperatures above 1000 ℃. Aiming at a better understanding of the structure–property relationship and the development of novel electronic devices, in recent years, the study of the nano-scaled ferroelectric materials has attracted immense attention. Novel synthesis techniques have been developed. Among them, wet-chemical methods are a promising alternative, because they can be better controlled from the molecular precursors to the final materials to give highly pure and homogeneous materials, and allow low reaction temperature to be used, the size and morphology of the particles to be controlled, and metastable phases to be prepared. There are two kinds of wet-chemical routes for the synthesis of perovskite nanocrystals. One is the precipitation method which obtains the precursors such as carbonate, hydroxide, oxalate, and dry gel by solution method and then sinters them to obtain the perovskite nanocrystals. Although the method is very simple and the reaction in solution can be operated even at room temperature, the agglomerations and grain growth are inevitable during calcination. The other one is the direct synthesis of perovskite nanostructures in solution, and much effort has been made on it in recent years. Hydrothermal method is one of the most popular approaches to obtain the perovskite nanostructures directly from solution, but the synthesis process is often conducted at elevated temperature (typically 100–280 ℃) and/or under relatively high pressure to improve the crystallinity of the products. To further simplify the process and lower the processing temperature and pressure, several routs have been achieved [4–12]. Even more, perovskite structured nanocrystals with much complicated compositions have been developed based on above research works to develop new functional ceramics [13–17]. However, the agglomerations are inevitable in fine grain sized powders, especially in the nanoparticles, and thus the pores are hard to eliminate thoroughly during sintering. To extend the application of nanoparticles in ceramic fabrication, this difficulty should be overcome thoroughly.

Barium zirconate titanate ($BaZr_xTi_{1-x}O_3$, BZT) based materials are important for potential applications such as piezoelectric transducers, DRAM, tunable microwave devices, and giant permittivity capacitors [18–21]. The three transition points and the three corresponding ε_r maxima of BZT materials can move closer together and coalesce into a single broad maximum at $x = 0.10$ while the zirconium content increases. After moving the broad maximum near room temperature, a high permittivity can be obtained. As a dielectric system with outstanding properties, the permittivity can be over 25 000 while withstand AC voltage is over 3.5 kV/mm [22]. As a lead-free piezoelectric system, it can have comparable piezoelectric coefficient to the PZT system with a maximum d_{33} of 600 pC/N, attributed to the coexisting tetragonal and rhombohedral phases near the morphotropic phase boundary (MPB) [23].

A high temperature over 1300 ℃ is often necessary for the sintering of BZT into dense ceramics. It is important economically to decrease the sintering temperature for the multiple layer devices, especially lower than 1150 ℃, to accommodate 3:7 Pd–Ag alloy or Ni inner electrodes [24]. Zinc oxide can be used as sintering aid because of its slight solubility in BZT bulk materials. After adding sintering aid such as $ZnO–Li_2O$, the sintering temperature can be lowered to around 1250 ℃ [22].

In order to control the ceramic properties, the processing of fabrication should be much fine. Here, we designed another sintering approach to ceramics at low temperature from nanoparticles. Excessive dopants, such as ZnO, were introduced into the BZT ($BaZr_{0.1}Ti_{0.9}O_3$ in this study) nanoparticles during synthesizing them. These dopants would be liberated again at high temperature on the surfaces of the nanoparticles as sintering aid homogenously, and can promote the densification during sintering.

2 Experimental procedure

Both the ZnO-doped BZT nanoparticles and pure BZT nanoparticles were directly synthesized at room temperature. The preparation of the powders was evolved from direct synthesis from solution (DSS) [25] under the circumstance in an enclosed mill jar. The analytical reagents, barium hydroxide octahydrate ($Ba(OH)_2·8H_2O$), zirconium nitrate pentahydrate ($Zr(NO_3)_4·5H_2O$), zinc nitrate hexahydrate ($Zn(NO_3)_2·6H_2O$), and tetrabutyl titanate ($Ti(OC_4H_9)_4$), were adopted as starting raw materials to prepare the ZnO-doped BZT nanoparticles and pure BZT nanoparticles. The Zn-doped titanium and zirconium (ZT) solution was obtained by dissolving 30.6 g $Ti(OC_4H_9)_4$, 4.3 g $Zr(NO_3)_4·5H_2O$, and 0.6 g $Zn(NO_3)_2·6H_2O$ into 100 mL

absolute ethanol. The alkaline earth source slurry was prepared by ball milling 31.6 g $Ba(OH)_2 \cdot 8H_2O$ in 50 mL ethanol for 4 h on the planet type ball mill. The Zn-doped ZT solution was added into the alkali slurry in the jar, with the pH value adjusted by ammonium hydroxide aqueous solution near 10, and then resealed for another 18 h milling at the rate of 200 rpm. After that, homogenous white slurry was obtained. The white slurry was air-dried and ZnO-doped BZT (~2 mol%) nanoparticles were synthesized. As a comparison, BZT nanoparticles were also obtained under the same synthesis process but without involving zinc nitrate hexahydrate as we reported recently [26]. Both the as-prepared 2 mol% ZnO-doped nanoparticles (sample 1) and the pure BZT nanoparticles added with 2 mol% ZnO as sintering aid (sample 0) were dry pressed into the cylinders and disks. The cylinder samples were employed for dilatometry measurements at a heating rate of 5 ℃/min from room temperature to 1300 ℃, and the disk samples were employed for sintering into ceramics at 1150 ℃ for 2 h.

All the samples were characterized at room temperature by X-ray diffraction (XRD) on a Philips X-ray diffractometer (model: X'Pert-Pro MPD) using Cu Kα radiation (40 kV, 30 mA). The microstructures of the samples were observed by scanning electron microscopy (SEM) on a Zeiss field-emission scanning electron microscope (model: Supra 55). In order to measure the dielectric properties, the ceramic disk samples were coated with silver paste on both surfaces, and sintered at 850 ℃ for 10 min. After that, their dielectric properties were measured from –60 to 130 ℃ (model No. HP4192A, Hewlett-Packard Co., Palo Alto, CA, USA).

3 Results and discussion

It is well known that the temperature of the ceramic sintering could be decreased with the grain size of ceramic powders, but this "size advantage" is very often limited by the strong agglomeration observed within the nanoparticles that results in low final density or high sintering temperature. To overcome the difficulty, it is necessary to develop a new approach to sintering the ceramics. Dopant addition is a way to overcome this problem, but then the effective dispersion of the dopant among the nanoparticles is another key point to solve. Generally, some dopants with high vapor pressure and/or low melting point and slightly solubility in bulk ceramics can be adopted as sintering aids, but it is not always effective for nanoparticles because they can hardly reach into the inevitable agglomerations. The sintering aids can hardly jam into the inner space of the agglomerations, and pores easily remain after sintering. We describe this process in Fig. 1(a). Fortunately, these dopants and impurities may have larger solubility in nanoparticles than that in bulk materials for the opening structure in nanomaterials. For example, Ba or Ti can have much more solubility in $BaTiO_3$ nanoparticles than in bulk materials [11,27]. This behavior is our designing clue for a new approach to ceramic sintering from nanoparticles. When excessive dopants or impurities are introduced into nanoparticles, they can be liberated on the surfaces of the nanoparticles homogenously from bulk for the exsolution during sintering, and can act as sintering aids. The process is shown in Fig. 1(b). Therefore, the sintering densification can be promoted greatly. In this study, we select BZT ceramic sintering as our target. Both the ZnO-doped BZT nanoparticles and the BZT

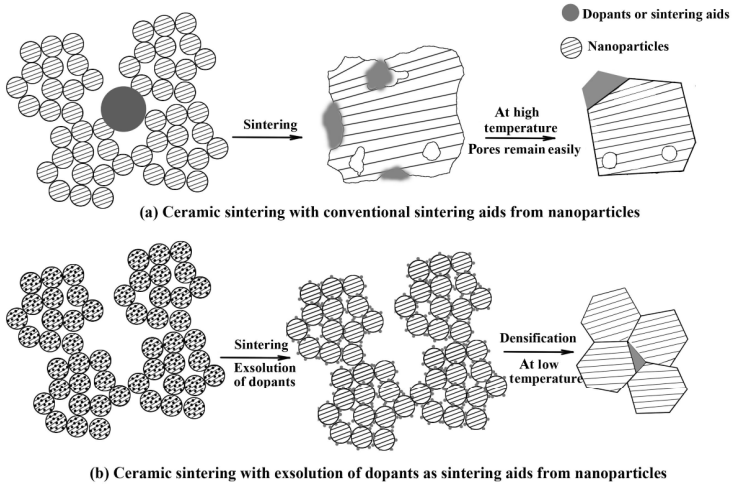

Fig. 1 Description of (a) conventional ceramic sintering and (b) strategy of the new approach from nanoparticles.

nanoparticles with the same amount of ZnO as sintering aid are sintered at 1150 ℃.

Zinc oxide can be used as sintering aid for sintering BZT ceramic because of its slight solubility in BZT bulk materials. It can be expected a potential large solubility in BZT nanoparticles although there are rare data in previous documents. BZT and ZnO-doped BZT nanoparticles were prepared under the same condition by direct synthesis method as we reported previously [26]. Both of them were synthesized at room temperature in the mill jar. Their morphologies are very similar as nanoparticles shown in Fig. 2, and the strong agglomerations with size of ~100 nm are observed. Their crystalline structures were checked by XRD as shown in Fig. 3 and confirmed as perfect perovskite. Both of them have a grain size of ~10 nm estimated by either SEM or XRD.

Although the peaks of impurity phase at 24°, 33°, and others are indexed as $BaCO_3$ (PDF No. 71-2394) in Fig. 3, they disappear after suitable annealing at a temperature over 700 ℃. The small amount of $BaCO_3$ and its different contents in the as-prepared samples possibly derive from the raw material barium hydroxide, which can react with CO_2 in air during its storage. $BaCO_3$ can be synthesized into the perovskite structure while releasing CO_2 at a temperature as low as 500–700 ℃, because the decrease of $BaCO_3$ phase is clearly observed [26]. There are slight differences between two XRD profiles of BZT nanoparticles and ZnO-doped one, except that the peaks of the latter shift towards to the left very slightly comparing with the former (e.g., near 55°, BZT 55.58° vs. ZnO-doped BZT 55.4°; near 65°, BZT 65.18° vs. ZnO-doped BZT 65.08°). The lattice cell of both as-prepared nanoparticles could expand distinctly comparing with their bulk materials due to both "size effects" and hydrogen interstitials introduced during synthesis. Their lattices have very open structure and have ability to contend more defects. Therefore, the lattice cell expansion caused by the doping of Zn ion in ZnO-doped BZT is not distinct as we expected, and we just observe a very slight left shift of the XRD peaks of ZnO-doped BZT comparing with that of pure BZT nanoparticles, although the results imply that Zn ion has already been in the lattice of the BZT in ZnO-doped sample 1.

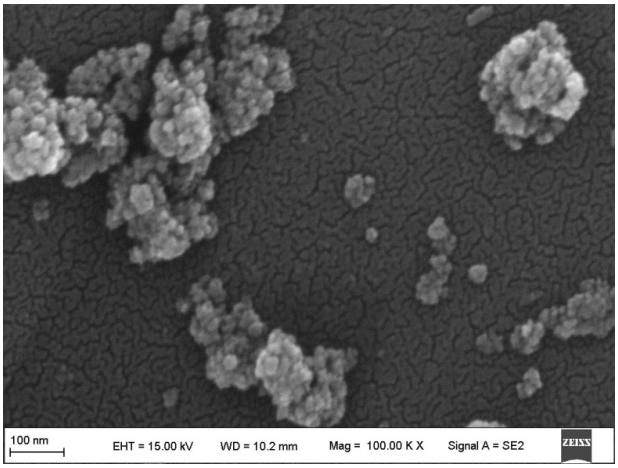

Fig. 2 SEM of ZnO-doped BZT nanoparticles.

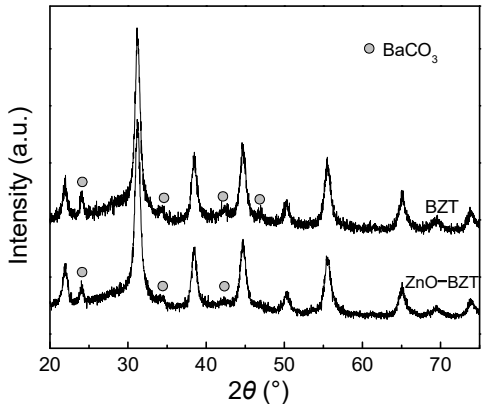

Fig. 3 XRD profile of as-prepared pure BZT and ZnO-doped BZT nanoparticles.

In order to compare the sintering characteristics of the above as-prepared nanoparticles, dilatometry measurements were done for the cylinders of the sample 0 and the sample 1 as shown in Fig. 4. The sample 1 (ZnO-doped BZT) has a distinct shrinkage over 1100 ℃ and tends to a constant at 1150 ℃, whereas the sample 0 (BZT with ZnO as additive) has a distinct shrinkage over 1200 ℃ and increases with the temperature till 1300 ℃. The ceramics were also sintered at 1150 ℃ for 2 h according to the type described in Fig. 1(b) with the sample 1, and according to the type described in Fig. 1(a) with the sample 0 as a comparison, respectively. The microstructures of the ceramics were observed by SEM.

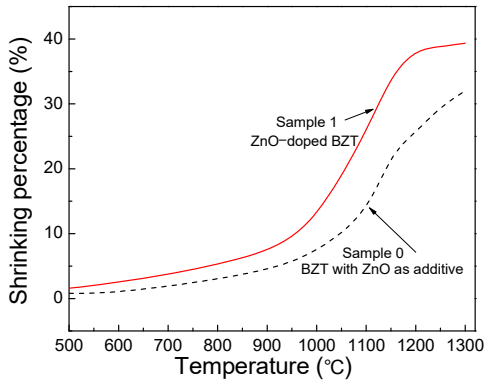

Fig. 4 Dilatometry measurements for the samples.

The dense ceramic structure of the sample 1 is clear shown in Fig. 5, and rather homogenous grains with the average size of 1 μm can be observed as well. The microstructures of the sample 0 and sample 1 were checked with the same magnification of 10k× as shown in Fig. 6 to compare their differences. Many pores and a secondary phase (indexed as ZnO by EDAX) are found in the sample 0, and the relative density is only 78%. On the contrary, pores can be rarely observed in the sample 1, and its relative density is as high as 99%. The average grain size of the sample 0 is only ~300 nm, but that of the sample 1 is much greater as ~1 μm. All of these observations are just in accordance with the strategy we propose as illustrated in Fig. 1.

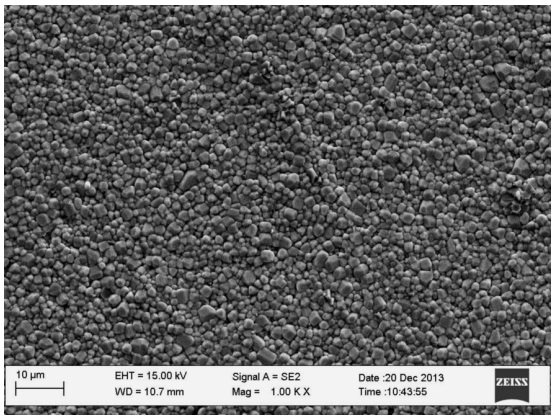

Fig. 5 SEM of the sample 1 with the dense structure and homogenous grain size.

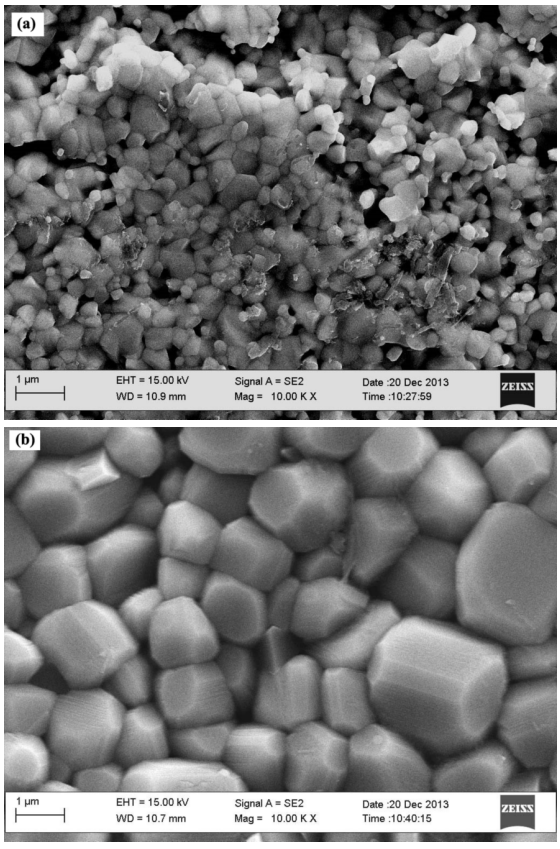

Fig. 6 SEM of the samples: (a) the sample 0, (b) the sample 1.

ZnO has a slight solubility less than ~1 mol% in $BaTiO_3$ based materials, and can be adopted as sintering aid to lower ceramic sintering temperature [28]. ZnO doped in $BaTiO_3$ based materials behaves as acceptor as

$$ZnO \rightarrow Zn''_{Ti} + V_O^{\bullet\bullet} + O_O^{\times}$$

Here, the oxygen vacancy is a deep acceptor in perovskite $BaTiO_3$ based materials. Because the sintering of $BaTiO_3$ based ceramics is often controlled by solid state sintering pattern, the mass transfer of the ions is tightly related with the point defects in the lattice. Oxygen vacancy decreases the energy of the transfer of each ion, and thus speeds up the mass transfer during sintering [29]. As we discuss here, the sintering of both the sample 0 and sample 1 can be promoted by Zn ions in the lattice, but the type of Fig. 1(b) in the sample 1 is much more effective than the type of Fig. 1(a) in the sample 0. Much more Zn ions could be incorporated in the lattice of the open structure of the nanomaterials in the sample 1 during the synthesis, and the doping of Zn ions could produce much more oxygen vacancies. Therefore, the bulk mass transfer among nanoparticles is improved during soaking time, and the sintering of the sample 1 is promoted greatly. Another reason is that excessive ZnO can be liberated from the lattice cell on the surface of each nanoparticle as sintering aid to promote sintering effectively. On the contrary, the added ZnO is hard to disperse homogenously in the sample 0, and ZnO could jam into the inner space of the agglomeration of BZT nanoparticles difficultly and pores easily remain after sintering. Therefore, the traditional sintering type in the sample 0 is not as effective as our new approach in the sample 1 for the nanoparticles.

The temperature dependence of dielectric properties of both the sample 0 and sample 1 is shown in Fig. 7. The sample 0 has a permittivity maximum about 3200 at 75 ℃, and a big loss about 0.17 because the ceramic is not dense enough. On the contrary, the sample 1 has a permittivity maximum as much as 6700 at 55 ℃ with a loss below 0.02, and thus the ceramic can be applied for ceramic capacitor. Comparing with the sample 0, the permittivity peak of the sample 1 has a shift to low temperature 55 ℃ from 75 ℃ due to the more

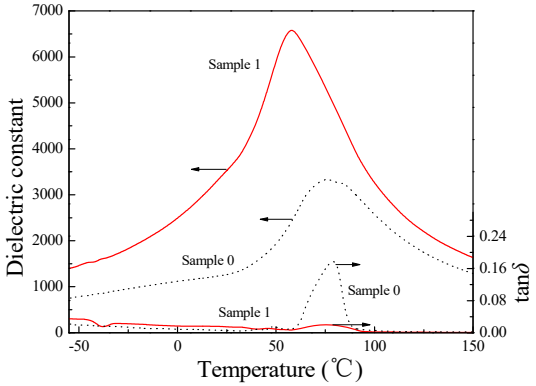

Fig. 7 Dielectric properties of the samples.

incorporation of Zn ions into the lattice cell in ZnO-doped BZT ceramic.

4 Conclusions

The perovskite structured BZT nanoparticles doped with 2 mol% ZnO can be synthesized with the grain size of ~10 nm at room temperature. Sintering of their green ware at the temperature as low as 1150 ℃ for 2 h, very dense ceramic can be obtained. As a comparison, sintering of the green ware of pure BZT nanoparticles with 2 mol% ZnO as sintering aid in the same condition, the porous BZT ceramic can be obtained. Therefore, the traditional sintering type as simply adding sintering aid is not effective for the sintering of the nanoparticles due to the agglomerations, while the approach we design is much more effective. During sintering of our approach, dopants incorporated into the lattice of the nanoparticles during their synthesis can introduce much more defects to promote the sintering. Moreover, the excessive dopants can be liberated again on the surfaces of the nanoparticles as sintering aids homogenously, and promote the sintering effectively.

Acknowledgements

The authors are grateful for the supports of Basic Key Program of Applied Basic Research of Science and Technology Commission Foundation of Hebei Province in China (Grant Nos. 14961108D and 15961005D) and Open Project of State Key Laboratory of New Ceramics and Fine Processing, Tsinghua University (No. KF201410).

References

[1] Fernández JF, Caballero AC, Durán P, *et al.* Improving sintering behavior of $BaTiO_3$ by small doping additions. *J Mater Sci* 1996, **31**: 975–981.

[2] Yang W-G, Zhang B-P, Ma N, *et al.* High piezoelectric properties of $BaTiO_3$–xLiF ceramics sintered at low temperatures. *J Eur Ceram Soc* 2012, **32**: 899–904.

[3] Polotai AV, Fujii I, Shay DP, *et al.* Effect of heating rates during sintering on the electrical properties of ultra-thin Ni–$BaTiO_3$ multilayer ceramic capacitors. *J Am Ceram Soc* 2008, **91**: 2540–2544.

[4] Suyama Y, Nagasawa M. Synthesis of single-crystal barium titanium isopropoxide complex to form barium titanate. *J Am Ceram Soc* 1994, **77**: 603–605.

[5] Urban JJ, Yun WS, Gu Q, *et al.* Synthesis of single-crystalline perovskite nanorods composed of barium titanate and strontium titanate. *J Am Chem Soc* 2002, **124**: 1186–1187.

[6] O'Brien S, Brus L, Murray CB. Synthesis of monodisperse nanoparticles of barium titanate: Toward a generalized strategy of oxide nanoparticle synthesis. *J Am Chem Soc* 2001, **123**: 12085–12086.

[7] Hernandez BA, Chang K-S, Fisher ER, *et al.* Sol–gel template synthesis and characterization of $BaTiO_3$ and $PbTiO_3$ nanotubes. *Chem Mater* 2002, **14**: 480–482.

[8] Pérez-Maqueda LA, Diánez MJ, Gotor FJ, *et al.* Synthesis of needle-like $BaTiO_3$ particles from the thermal decomposition of a citrate precursor under sample controlled reaction temperature conditions. *J Mater Chem* 2003, **13**: 2234–2241.

[9] Urban JJ, Spanier JE, Ouyang L, *et al.* Single-crystalline barium titanate nanowires. *Adv Mater* 2003, **15**: 423–426.

[10] Niederberger M, Pinna N, Polleux J, *et al.* A general soft-chemistry route to perovskites and related materials: Synthesis of $BaTiO_3$, $BaZrO_3$, and $LiNbO_3$ nanoparticles. *Angew Chem Int Edit* 2004, **43**: 2270–2273.

[11] Wada S, Tsurumi T, Chikamori H, *et al.* Preparation of nm-sized $BaTiO_3$ crystallites by a LTDS method using a highly concentrated aqueous solution. *J Cryst Growth* 2001, **229**: 433–439.

[12] Qi J, Li L, Wang Y, *et al*. Preparation of nanoscaled $BaTiO_3$ powders by DSS method near room temperature under normal pressure. *J Cryst Growth* 2004, **260**: 551–556.

[13] Chen CF, Reagor DW, Russell SJ, *et al.* Sol–gel processing and characterizations of a $Ba_{0.75}Sr_{0.25}Ti_{0.95}Zr_{0.05}O_3$ ceramic. *J Am Ceram Soc* 2011, **94**: 3727–3732.

[14] Qi JQ, Wang Y, Chen WP, *et al.* Perovskite barium zirconate titanate nanoparticles directly synthesized from solutions. *J Nanopart Res* 2006, **8**: 959–963.

[15] Mathur S, Shen H, Lecerf N, *et al*. Sol–gel synthesis route for the preparation of $Y(Ba_{1-x}Sr_x)_2Cu_4O_8$ superconducting oxides. *J Sol–Gel Sci Technol* 2002, **24**: 57–68.

[16] Rabuffetti FA, Brutchey RL. Local structural distortion of $BaZr_xTi_{1-x}O_3$ nanocrystals synthesized at room temperature. *Chem Commun* 2012, **48**: 1437–1439.

[17] Rabuffetti FA, Lee JS, Brutchey RL. Low temperature synthesis of complex $Ba_{1-x}Sr_xTi_{1-y}Zr_yO_3$ perovskite nanocrystals. *Chem Mater* 2012, **24**: 3114–3116.

[18] Yu Z, Ang C, Guo R, *et al*. Piezoelectric and strain properties of $Ba(Ti_{1-x}Zr_x)O_3$ ceramics. *J Appl Phys* 2002, **92**: 1489.

[19] Wu TB, Wu CM, Chen ML. Highly insulative barium zirconate–titanate thin films prepared by rf magnetron sputtering for dynamic random access memory applications. *Appl Phys Lett* 1996, **69**: 2659–2662.
[20] Tang XG, Wang J, Wang XX, *et al.* Effects of grain size on the dielectric properties and tunabilities of sol–gel derived $Ba(Zr_{0.2}Ti_{0.8})O_3$ ceramics. *Solid State Commun* 2004, **131**: 163–168.
[21] Hennings D, Schnell A, Simon G. Diffuse ferroelectric phase transitions in $BaTi_{1-y}Zr_yO_3$. *J Am Ceram Soc* 1982, **65**: 539–544.
[22] Qi J, Gui Z, Wang Y, *et al.* Doping behavior of ytterbium oxide in $Ba(Ti_{1-y}Zr_y)O_3$ dielectric ceramics. *J Mater Sci Lett* 2002, **21**: 405–406.
[23] Liu W, Ren X. Large piezoelectric effect in Pb-free ceramics. *Phys Rev Lett* 2009, **103**: 257602.
[24] Kishi H, Mizuno Y, Chazono H. Base-metal electrode-multilayer ceramic capacitors: Past, present and future perspectives. *Jpn J Appl Phys* 2003, **42**: 1–15.
[25] Qi JQ, Peng T, Hu YM, *et al.* Direct synthesis of ultrafine tetragonal $BaTiO_3$ nanoparticles at room temperature. *Nanoscale Res Lett* 2011, **6**: 466.
[26] Qi JQ, Wang XH, Zhang H, *et al.* Direct synthesis of barium zirconate titanate (BZT) nanoparticles at room temperature and sintering of their ceramics at low temperature. *Ceram Int* 2014, **40**: 2747–2750.
[27] Qi JQ, Sun L, Du P, *et al.* Stoichiometry of $BaTiO_3$ nanoparticles. *J Nanopart Res* 2010, **12**: 2605–2609.
[28] Caballero AC, Fernández JF, Moure C, *et al.* Grain growth control and dopant distribution in ZnO-doped $BaTiO_3$. *J Am Ceram Soc* 1998, **81**: 939–944.
[29] Levi RD, Tsur Y. The effect of oxygen vacancies in the early stages of $BaTiO_3$ nanopowder sintering. *Adv Mater* 2005, **17**: 1606–1608.